Neurotherapeutics (2023) 20:1835–1846
https://doi.org/10.1007/s13311-023-01429-6

ORIGINAL ARTICLE

Intravenous Administration of an AAV9 Vector Ubiquitously Expressing *C1orf194* Gene Improved CMT-Like Neuropathy in *C1orf194*$^{-/-}$ Mice

Zongrui Shen[1] · Meiyi Li[1] · Fei He[1] · Cheng Huang[1] · Yingchun Zheng[1] · Zhikui Wang[1] · Shunfei Ma[1] · Li Chen[1] · Zhengshan Liu[3] · Hui Zheng[2] · Fu Xiong[1,4,5]

Accepted: 19 August 2023 / Published online: 16 October 2023

Abstract

Charcot-Marie-Tooth (CMT) disease, also known as hereditary motor sensory neuropathy, is a group of rare genetically heterogenous diseases characterized by progressive muscle weakness and atrophy, along with sensory deficits. Despite extensive pre-clinical and clinical research, no FDA-approved therapy is available for any CMT type. We previously identified *C1ORF194*, a novel causative gene for CMT, and found that both *C1orf194* knock-in (I121N) and knockout mice developed clinical phenotypes similar to those in patients with CMT. Encouraging results of adeno-associated virus (AAV)-mediated gene therapy for spinal muscular atrophy have stimulated the use of AAVs as vehicles for CMT gene therapy. Here, we present a gene therapy approach to restore *C1orf194* expression in a knockout background. We used *C1orf194*$^{-/-}$ mice treated with AAV serotype 9 (AAV9) vector carrying a codon-optimized WT human *C1ORF194* cDNA whose expression was driven by a ubiquitously expressed chicken β-actin promoter with a CMV enhancer. Our preclinical evaluation demonstrated the efficacy of AAV-mediated gene therapy in improving sensory and motor abilities, thus achieving largely normal gross motor performance and minimal signs of neuropathy, on the basis of neurophysiological and histopathological evaluation in *C1orf194*$^{-/-}$ mice administered AAV gene therapy. Our findings advance the techniques for delivering therapeutic interventions to individuals with CMT.

Keywords Charcot-Marie-Tooth disease · *C1orf194* · Adeno-associated virus

Introduction

Charcot-Marie-Tooth (CMT) disease—a group of rare inherited neuromuscular disorders estimated to affect approximately 1 in 1,200 to 10,000 individuals—is characterized by progressive motor and sensory peripheral neuropathy [1, 2]. Since the discovery of PMP22 duplication as the cause of CMT1A in 1999, more than 100 genes have been linked to CMT, making it a highly heterogeneous group of disorders. Dominant intermediate-type CMT (DI-CMT) accounts for about 4% of all CMT cases and is characterized by axonal degeneration, loss of the myelin sheath, decreased compound muscle action potential (CMAP) amplitude, and intermediate (25–45 m/s) motor nerve conduction velocity (NCV).

C1ORF194, also known as *CFAP276*, is a gene of unknown function. We previously reported that C1orf194 may function as a mitochondria-associated endoplasmic reticulum (ER) membrane (MAM) protein in CMT. Proteomics analysis of the sciatic nerve in C1orf194(p.I121N)

✉ Hui Zheng
82142953@qq.com

✉ Fu Xiong
xiongfu@smu.edu.cn

1 Department of Medical Genetics, Experimental Education/Administration Center, School of Basic Medical Sciences, Southern Medical University, Guangzhou, China

2 Department of Neurology, The First School of Clinical Medicine, Nanfang Hospital, Southern Medical University, Guangzhou, China

3 Division of Translational Neuroscience in Schizophrenia, Department of Psychiatry, University of Texas Southwestern Medical Center, Dallas, TX 75390, USA

4 Guangdong Provincial Key Laboratory of Single Cell Technology and Application, Guangzhou, Guangdong, China

5 Department of Fetal Medicine and Prenatal Diagnosis, Zhujiang Hospital, Southern Medical University, Guangzhou, China

knock-in mice has revealed upregulation of multiple calmodulins [3]. Further studies have indicated that C1ORF194 may function as a calmodulin, interacting with calcium channel proteins and influencing calcium transport between the endoplasmic reticulum and mitochondria. Mutated C1ORF194 disrupts intracellular calcium homeostasis, thus leading to CMT. We previously identified two missense mutations in C1ORF194 that give rise to two distinct CMT phenotypes: intermediate and demyelinating forms of CMT caused by p.I122N and p.K28I mutations, respectively. Patients with the *C1ORF194* mutation are characterized primarily by symmetrical distal muscle atrophy, progressive muscle weakness, sensory loss, and diminished tendon reflexes, accompanied by abnormal pathological and electrophysiological examination findings [3]. We generated the first *C1ORF194* knock-in and knockout mouse lines, which allowed us to establish the relationship between the loss of *C1orf194* and DI-CMT-like phenotype [3, 4]. These mouse models were generated on a C57BL/6J genetic background and recapitulated aspects of CMT neuropathy, such as demyelination and loss of motor neurons. Currently, we are investigating the precise molecular function of C1ORF194 and exploring various treatment approaches for CMT caused by the C1orf194 mutation [3].

CMT is a chronic disease characterized by slow progression [5–7]. No therapeutic options are available to reverse the course of CMT, and the typical clinical approach involves symptomatic and supportive treatments [8]. Some individuals require forearm crutches or canes for gait stability, whereas fewer than 5% of individuals require wheelchairs. Daily heel cord stretching exercises are recommended to prevent Achilles tendon shortening, and gripping exercises can help with hand weakness [9]. Exercise is encouraged within the capability of the individual, and many individuals remain physically active [10]. Orthopedic surgery may be required to correct severe pes cavus deformity [11]. Surgery is sometimes required for hip dysplasia [12]. The cause of any pain should be identified as accurately as possible. Recommended protocols include muscle strengthening, aerobic conditioning, stretching, and exercise for posture and balance [10, 13, 14].

In this study, we utilized an adeno-associated virus serotype 9 (AAV9) vector to deliver a human *C1ORF194* gene to neuronal and non-neuronal cells in *C1orf194*$^{-/-}$ mice, a mouse model of DI-CMT. The gene therapy restored C1orf194 expression, and led to significant improvements in gross motor performance, peripheral axon function, and histopathological phenotypes. The efficacy of AAV9-mediated C1ORF194 delivery was demonstrated in the *C1orf194*$^{-/-}$ mouse model, thus highlighting its potential function as a promising treatment approach for CMT. The *C1orf194*$^{-/-}$ mouse model displayed motor and sensory defects, accompanied by pathophysiologic changes in the sciatic nerve after the age of 4 months, and eventual development of a severe intermediate CMT phenotype. However, AAV9-mediated gene therapy effectively promoted and enhanced motor performance and peripheral axon function, and ameliorated histopathological phenotypes in the mouse model, thus highlighting the potential of AAV9-mediated C1ORF194 delivery to serve as an efficacious strategy for CMT treatment.

Results

AAV9-*C1ORF194* Gene Therapy Strategy

The *C1orf194*$^{-/-}$ mice developed a severe intermediate form of the CMT disease phenotype after reaching 4 months of age. This phenotype was characterized by noticeable motor and sensory defects, as well as pathophysiologic changes in the sciatic nerve [3, 4]. Therefore, we utilized the *C1orf194*$^{-/-}$ mice as a proof-of-concept preclinical model for gene-addition therapy in treating DI-CMT. Our approach was based on an AAV9 vector carrying a codon-optimized wild-type (WT) human *C1ORF194* cDNA driven by a ubiquitously expressed chicken β-actin promoter with a CMV enhancer. To assess the effectiveness of this virally mediated gene-addition strategy, we administered a single intravenous injection of AAV9-*C1ORF194* (5 × 10 [12] VG, approximately 250μL) to the mice at 45 days post-birth (Fig. 1).

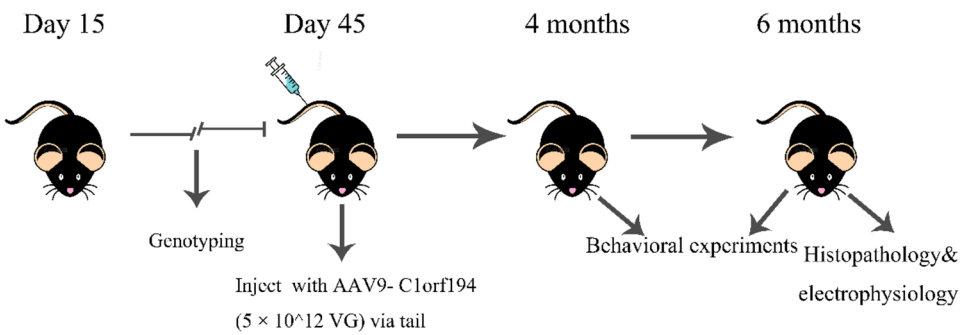

Fig. 1 Brief diagram of the study

Restoration of C1orf194 Protein Expression in the Sciatic Nerve After AAV9-*C1ORF194* Treatment

The protein expression levels of C1orf194 in the sciatic nerve were restored after treatment with AAV9-*C1ORF194*. We analyzed protein expression levels in the sciatic nerve through western blotting, which revealed a complete absence of C1orf194 protein in untreated *C1orf194*$^{-/-}$ mice (Fig. 2A, lanes 6–8). However, in the AAV9-*C1ORF194* treated mice, C1orf194 was detected at slightly lower levels than observed in WT mice (Fig. 2A, B).

AAV9-*C1ORF194* Gene Therapy Rescues Muscle Strength and Motor Coordination in *C1orf194*$^{-/-}$ Mice

To evaluate the effects of the treatment on muscle strength, we performed grip strength, rotarod, and running wheel tests in AAV9-*C1ORF194*-treated mice compared with untreated *C1orf194*$^{+/+}$ (WT) and *C1orf194*$^{-/-}$ mice. Motor symptoms in *C1orf194*$^{-/-}$ mice began to manifest at 4 months of age and worsened with age [3, 4]. Therefore, in this study, untreated *C1orf194*$^{+/+}$ (WT), *C1orf194*$^{-/-}$ mice (Control), and AAV9-*C1ORF194*-treated *C1orf194*$^{-/-}$ (treated) mice were tested for muscle strength at 4 and 6 months of age.

In the hind limb test, 6-month-old WT mice naturally extended their hind limbs and tried to escape. In contrast, *C1orf194*$^{-/-}$ mice were completely unable to extend their hind limbs, which drooped without application of force. However, in the AAV9-*C1ORF194* gene therapy group, the mice were able to naturally extend their hind limbs, thus showing some improvement over the condition of the *C1orf194*$^{-/-}$ mice, which were unable to extend their hind limbs at all (Fig. 2C, D).

In the rotarod test, at 4 months of age, *C1orf194*$^{-/-}$ mice remained on the rotating rod for shorter durations, thus indicating motor coordination deficits. However, after gene therapy, the *C1orf194*$^{-/-}$ mice remained on the rotarod for a longer duration, until the experiment was halted. The gene therapy-treated mice demonstrated motor coordination comparable to that of WT mice (Fig. 3A).

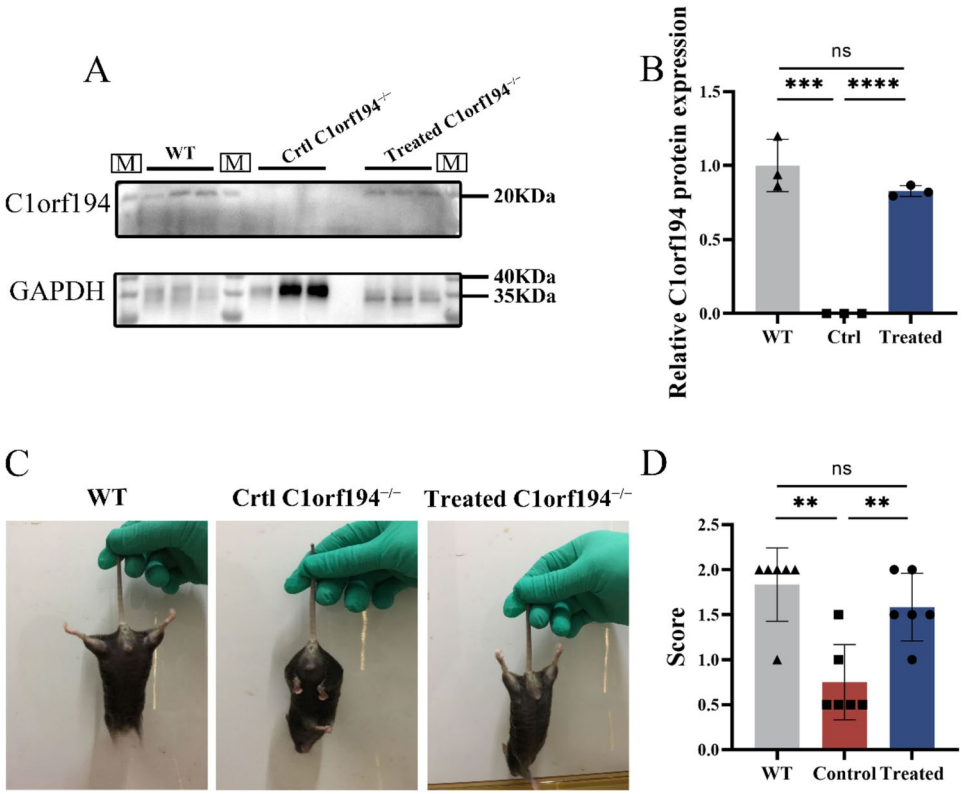

Fig. 2 Restoration of sciatic nerve C1orf194 protein levels with AAV9-*C1ORF194* therapy. In mice at 6 months of age, C1orf194 protein levels were evaluated through western blotting analysis of whole protein lysates extracted from the sciatic nerve after treatment with AAV9-*C1ORF194* therapy. **A** The accompanying figure illustrates a representative western blot, wherein C1orf194 is detected as a distinct band at 19 kDa. This band is observed in WT untreated mice (lanes 2–4), *C1orf194*$^{-/-}$ untreated mice (lanes 6–8), and *C1orf194*$^{-/-}$ treated mice (lanes 10–12). Lanes 1, 5, and 13 contain molecular weight reference. **B** C1orf194 levels were normalized to GAPDH as a loading control, and calculations were performed with WT untreated mice as a reference. This normalization method ensured accurate comparison and analysis of C1orf194 expression across different samples. **C** Results of hindlimb extension test. **D** Statistical results of hindlimb extension tests

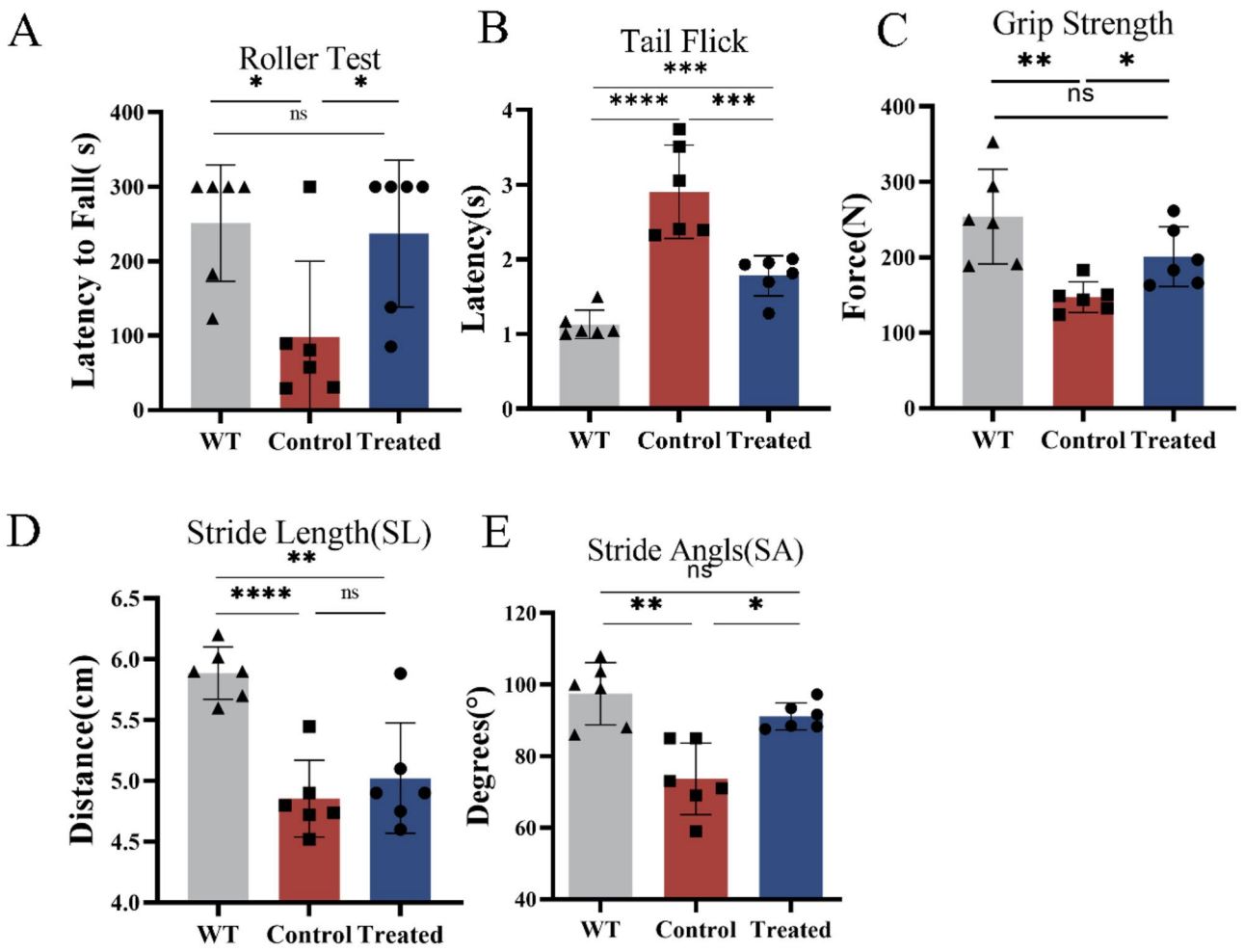

Fig. 3 Behavioral tests detecting motor and sensory defects in WT, untreated *C1orf194*$^{-/-}$ mice, and treated *C1orf194*$^{-/-}$ mice at 4 months old. Behavioral tests were conducted to assess motor and sensory impairments in 4-month-old wild-type (WT) mice, untreated *C1orf194*$^{-/-}$ mice, and treated *C1orf194*$^{-/-}$ mice. This test was aimed at detecting any abnormalities or deficiencies in hindlimb extension and overall functionality. **A** Limb movement evaluated with roller tests. **B** Sensitivity measured with tail-flicking tests. **C** Limb movement evaluated using grip strength tests. **D**, **E** Stride angle and length in different groups of mice

In the grip strength test, mice treated with AAV9-*C1ORF194* gene therapy exhibited stronger muscle performance (Fig. 3B).

In the tail-flick test, significant differences in pain sensitivity were observed among the groups of 4-month-old mice. However, the mice treated with AAV9-*C1ORF194* gene therapy did not show superior effects (Fig. 3C).

The gait characteristics of the mice were assessed with footprint analysis. At 4 months of age, *C1orf194*$^{-/-}$ mice exhibited shorter step length and smaller step angle. However, significant improvements in locomotor performance were observed in mice treated with AAV9-*C1ORF194*. Compared with *C1orf194*$^{-/-}$ mice, the treated *C1orf194*$^{-/-}$ mice showed noticeable improvements in step length and step angle (Fig. 3D, E). The schematic representation of the footprint analysis is shown in Fig. 4F.

Continued assessment of the behavioral performance of the three groups of mice at 6 months of age indicated that the effects of AAV9-*C1ORF194* gene therapy were more pronounced (Fig. 4A–E).

Nerve Conduction Velocity Is Improved by AAV9-*C1ORF194*

C1orf194$^{-/-}$ mice exhibited diminished NCV and CMAP amplitudes (Fig. 5A). However, after intravenous injection of AAV9-*C1ORF194* in *C1orf194*$^{-/-}$ mice, a significant improvement in NCV was observed at 6 months of age (Fig. 5B, C).

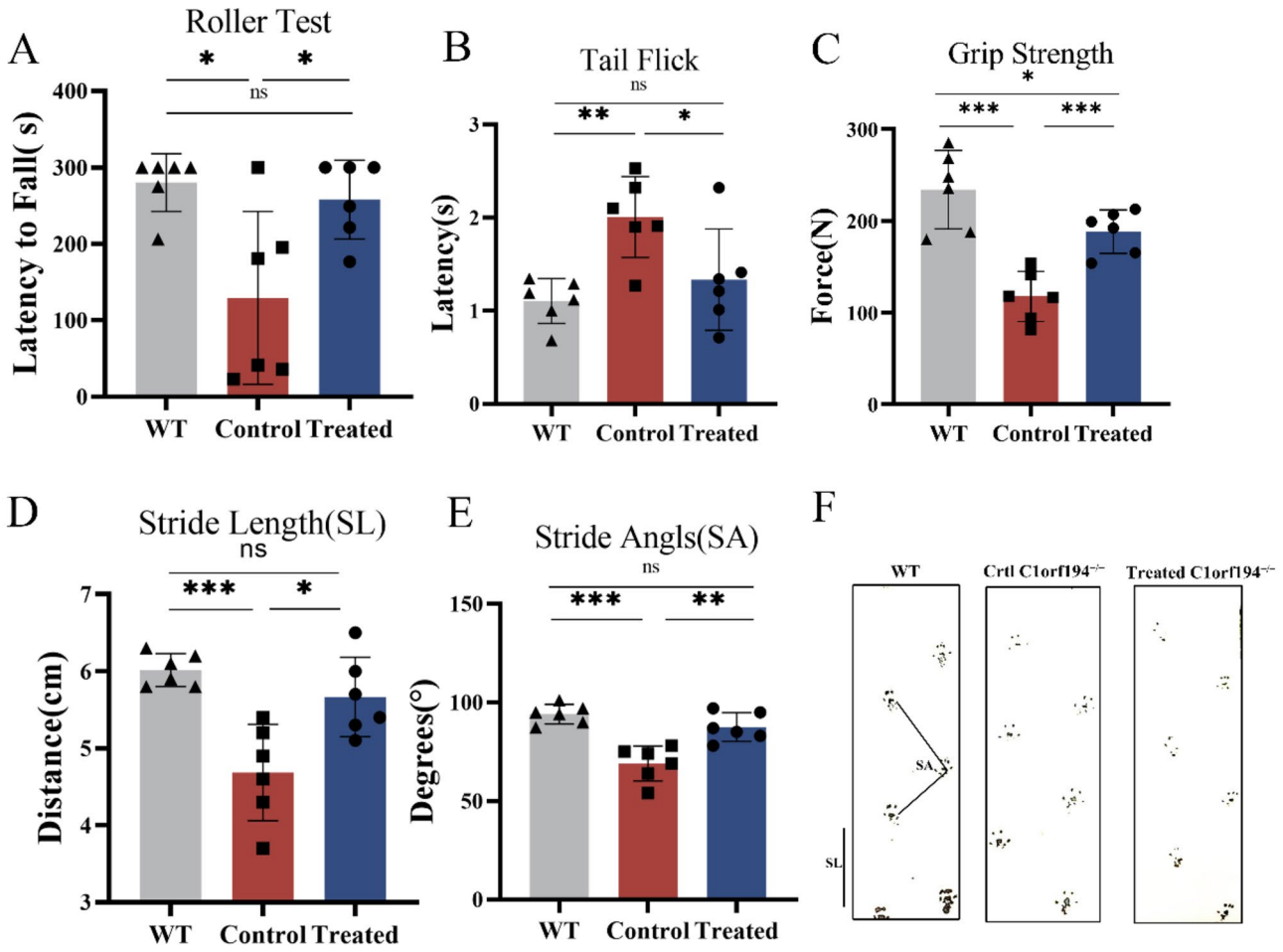

Fig. 4 Behavioral tests detecting motor and sensory defects in WT, untreated *C1orf194*$^{-/-}$ mice, and treated *C1orf194*$^{-/-}$ mice at 6 months old. **A** Limb movement evaluated with roller tests. **B** Sensitivity measured with tail-flicking tests. **C** Limb movement evaluated with grip strength tests. **D**, **E** Stride angle and length in different groups of mice. **F** Typical footprints of transgenic mice in the gait experiments

AAV9-*C1ORF194* Gene Therapy Mitigates Peripheral Nerve Degeneration and Muscle Atrophy

Hematoxylin and eosin (H&E) staining of the gastrocnemius muscle revealed the presence of necrotic, atrophied, and rimmed vacuoles in untreated *C1orf194*$^{-/-}$ mice (Fig. 6A). However, this pathological condition markedly improved in *C1orf194*$^{-/-}$ mice treated with AAV9-*C1ORF194* (Fig. 5A). Furthermore, Nissl staining of the lumbar spinal cord highlighted the intact motor neurons with abundant dendrites in the anterior horn of WT mice. In contrast, *C1orf194*$^{-/-}$ mice and AAV9-*C1ORF194*-treated *C1orf194*$^{-/-}$ mice showed low content of Nissl bodies, lightly stained, and fewer motor neurons (Fig. 6B, C).

Additionally, we examined ultra-thin sections of the sciatic nerve through transmission electron microscopy to evaluate histopathologic changes in myelination and axon structure. In *C1orf194*$^{-/-}$ mice, we observed an increase in myelin thickness and the presence of gaps in the myelin sheath of peripheral nerve fibers, indicative of chronic myelin compaction loss (Fig. 7B). These pathological changes were significantly ameliorated in the mice treated with AAV9-*C1ORF194* gene therapy (Fig. 7C). In addition, compared with *C1orf194*$^{-/-}$ mice, mice treated with AAV9-*C1ORF194* showed smaller sciatic nerve fiber diameters and a significant improvement in the abnormal thickening of the myelin sheath (Fig. 7D, E). The decrease in the G ratio (calculated by dividing axon diameter by fiber diameter) indicated an increase in myelin sheath thickness in the sciatic nerve of *C1orf194*$^{-/-}$ mice. However, mice treated with AAV9-*C1ORF194* showed a significant increase in the G ratio, thereby suggesting a further improvement in myelin sheath thickness (Fig. 7F). Quantitative analysis revealed a higher demyelination rate in the sciatic nerve of *C1orf194*$^{-/-}$ mice than WT mice and AAV9- *C1ORF194*-treated *C1orf194*$^{-/-}$ mice (Fig. 7G).

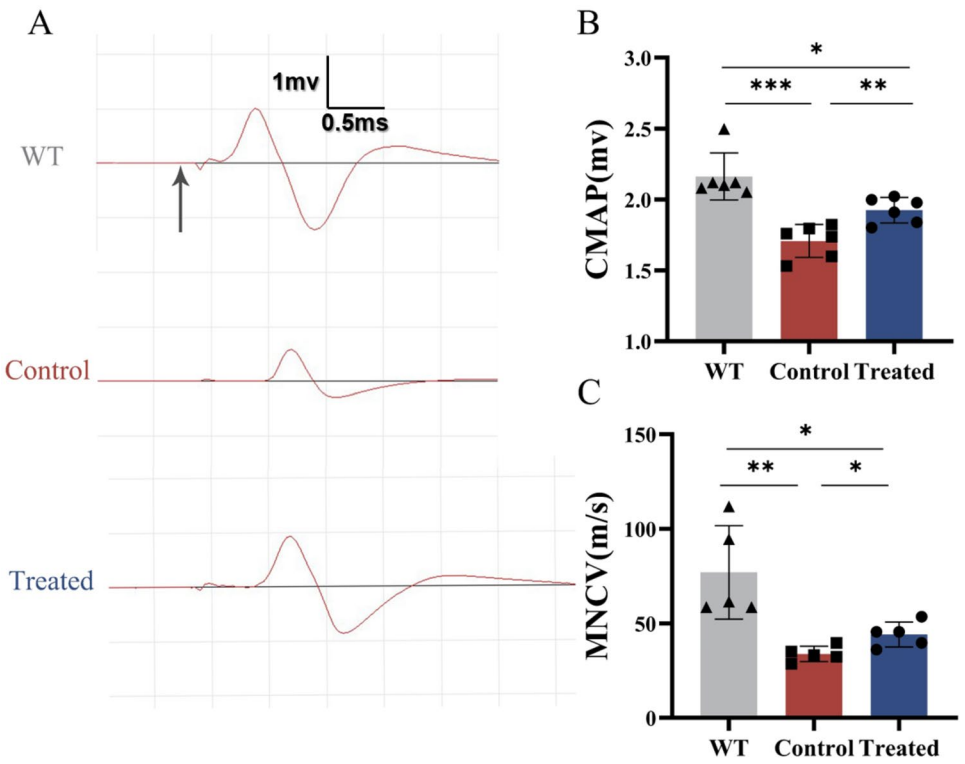

Fig. 5 Nerve conduction velocity is improved by AAV9-*C1ORF194*. **A** Representative traces from electrophysiologic recordings of the sciatic nerve in mice. The black arrow indicates the stimulation point in the distal nerve. X-axis represents time, and the Y-axis represents amplitude. **B**, **C** Statistical analysis of CMAP and NCV in transgenic mice

Discussion

Our study demonstrated the efficacy and tolerability of AAV9-mediated *C1ORF194* gene therapy in *C1orf194*$^{-/-}$ mice. In our previous study, we reported two families with *C1ORF194* missense mutations that showed distinct CMT-related symptoms [4]. In previous studies, both *C1orf194* knock-in (I121N) and *C1orf194*$^{-/-}$ mice were found to develop clinical phenotypes similar to those of patients with CMT [3, 4]. Thus, *C1orf194*$^{-/-}$ mice are a valid disease model for CMT. However, the underlying mechanism linking C1orf194 mutations and CMT development remains to be elucidated. The findings of this study have substantial clinical translation value. First, the successful utilization of gene therapy has effectively improved the motor and sensory capabilities of *C1orf194*$^{-/-}$ mice, thus supporting the potential application of this treatment approach in human patients with DI-CMT. This study provides compelling evidence of the promising therapeutic effects of AAV9-*C1ORF194* gene therapy in a mouse model, thereby establishing a solid groundwork for future clinical investigations and treatment trials.

In this study, mice with *C1orf194*$^{-/-}$ mutations were treated with a single intravenous injection of AAV9 vector carrying a codon-optimized WT human *C1ORF194* cDNA. The treatment successfully restored C1orf194 protein expression in the sciatic nerve, and the treated mice had detectable levels of C1orf194 protein. The therapeutic effects of AAV9-*C1ORF194* gene therapy were assessed through various evaluations, which revealed significant improvements in muscle performance, motor coordination, and locomotor performance in treated mice, in contrast to untreated mice. Furthermore, treated mice showed improvements in nerve conduction velocity and compound muscle action potential amplitudes, thus indicating the potential of this gene therapy for restoring peripheral nerve function. Histopathological analysis demonstrated that untreated mice displayed pathological changes, including necrotic, atrophied muscle fibers, and diminished Nissl bodies in the spinal cord. However, these pathological conditions were markedly ameliorated after mice were treated with AAV9-*C1ORF194* gene therapy. Transmission electron microscopy analysis further confirmed the therapeutic potential of this gene therapy by revealing improvements in myelin sheath structure, thereby suggesting a possible reduction in peripheral nerve degeneration and abnormal myelin thickness.

Gene therapy has emerged as a promising approach to treating monogenic developmental neurological disorders [15–18]. In our study, C1orf194 expression in the sciatic nerve in mice was restored after AAV9-*C1ORF194* treatment. AAV9, one of the most actively investigated gene therapy vectors, enables efficient gene delivery to various tissues, including skeletal and cardiac muscle [10, 19–21]. Immune responses induced by AAV9-mediated gene therapies have been extensively studied pre-clinically and clinically with minor concerns being raised [22]. However,

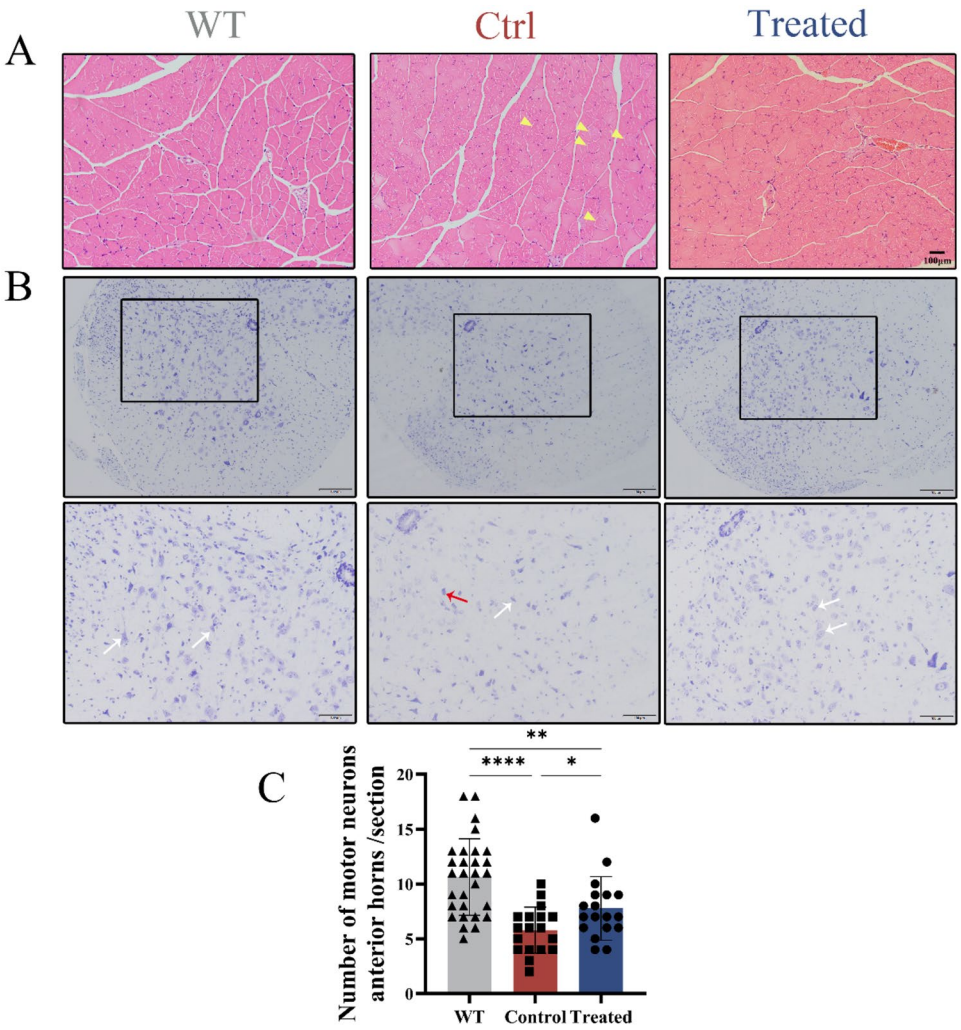

Fig. 6 Diminished H&E staining and Nissl staining pathology in AAV9-*C1ORF194*-treated mice. **A** H&E staining of gastrocnemius muscle tissue sections from untreated WT mice, untreated *C1orf194*$^{-/-}$ mice, and AAV9-*C1ORF194*-treated mice. Atrophy, abnormal muscle cell shape, and the presence of rimmed vacuoles (yellow arrowhead) increased in untreated *C1orf194*$^{-/-}$ mice. **B** Spinal cord anterior horn motor neurons with high content of Nissl bodies in the cytoplasm are indicated by a white arrow. Lightly stained nuclei and unclear nucleoli, and low content of Nissl bodies (red arrow) are observed in the *C1orf194*$^{-/-}$ mice. **C** Statistical analysis of Nissl bodies

despite the numerous advantages of AAV in gene therapy, several limitations must be considered. First, AAV has a limited ability to deliver large genes or gene clusters. Second, the transduction efficiency of AAV varies across different tissues and cell types, and some tissues or cells show relatively lower transfection rates. It is important to mention that patients should be first tested negative for pre-existing AAV neutralizing antibodies for being eligible to AAV-treatments. Onasemnogene (also known as onasemnogene abeparvovec, Zolgensma, AVXS-101) is an AAV9-mediated gene therapy drug approved in 2019 for the treatment of SMA. The drug is delivered to the patients intravenously [23]. Regarding safety concerns associated with AAV, recent reports have described two children who died after Zolgensma treatment, because of acute liver failure. These findings highlight the potential risks of AAV therapy, particularly in the context of liver function-related diseases. The occurrence of these tragic events underscores the need for further research and evaluation to ensure the safety of AAV-based treatments. In our experiments, we did not observe any pathological changes in the organs of the mice, and by the end of the study, no tumorigenic or teratogenic phenomena were detected in the mice in the experimental group. However, despite these findings, close monitoring and reporting of any adverse events will be essential when considering the translation of our research to the clinical setting, to ensure patient safety.

In our study, treatment effects were already evident in 4-month-old mice, particularly in rotarod and grip strength tests. The effects became more pronounced when the mice were 6 months old.

In conclusion, transduction of neural cells by the intravenously delivered AAV9-*C1ORF194* improved rotarod test performance in model mice, and rescued the pathophysiology of neuronal populations in the spinal cord. The improved performance was particularly evident in the roller and tail flick tests. Although the reason why other locomotor functions did not change remains unclear, the observed improvements may be attributable to amelioration

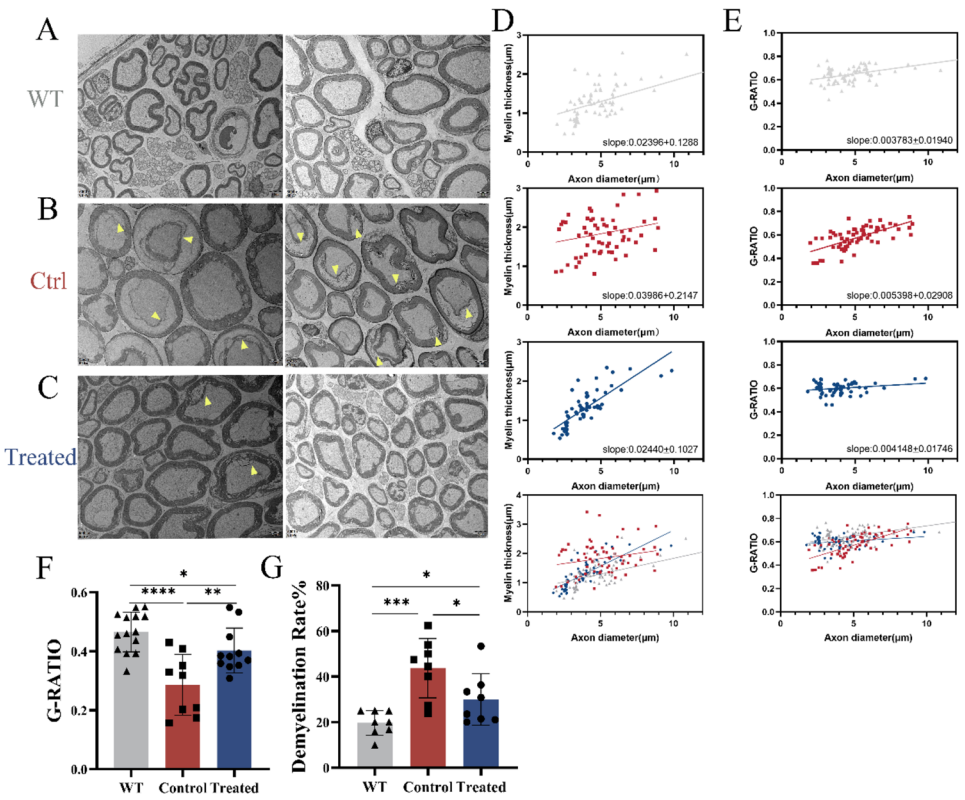

Fig. 7 Transmission electron microscopy analysis of the sciatic nerve. **A**–**C** Transmission electron micrographs of the sciatic nerves of WT, *C1orf194*$^{-/-}$ untreated mice, and *C1orf194*$^{-/-}$ treated mice. Representative electron micrographs at 5000× magnification are shown. Yellow arrowheads indicate myelin breakdown. **D**, **E** Scatterplots of G ratios and myelin thickness. The formula for calculating the G ratio which was the ratio of axon diameter to fiber diameter was as follows: G ratio=axon diameter/nerve fiber diameter. The formula for calculating the average myelin thickness was the difference between the fiber radius and the axon radius. **F** G ratio statistics reflecting changes in the thickness of the myelin sheath. **G** Demyelination rate of mice sciatic nerve. Demyelination rate = (Total number of demyelinated fibers/Total number of fibers) × 100

of psychomotor functions. However, even though the behavioral and pathological deficits in the *C1orf194*$^{-/-}$ mice were not fully corrected, the AAV9 delivery of *C1ORF194* was largely successful. Whether this approach could be further optimized is worthy of exploration. In future studies, we will optimize the injectable dose, dosing method, and dosing period. During tail vein injections in mice, the closed blood-nerve barrier, a characteristic of rodents, can impede the transfer of genes to the nervous system. This limitation may have hindered our study from achieving optimal conditions for gene delivery. During tail vein injections in mice, it is crucial to acknowledge that the closed blood-nerve barrier, inherent to rodents, can impede gene transfer to the nervous system, potentially affecting the optimal conditions for gene delivery in our study. However, our study revealed remarkable enhancements in the motor and sensory capabilities of *C1orf194*$^{-/-}$ mice after AAV9-*C1ORF194* gene therapy. These findings indicate that, despite the presence of a closed blood-nerve barrier, the potential exists for gene transduction and therapeutic effects on Schwann cells or other mechanisms within the peripheral nervous system. Schwann cells play crucial roles in the nervous system, including providing support and insulation, promoting nerve regeneration, and participating in the remyelination process. In our study, the improvements observed in the G ratio and nerve conduction velocities are attributable to the transduction of Schwann cells. Schwann cells facilitate remyelination or remyelination repair, thereby contributing to the observed enhancements in these parameters.

In our study, we performed tail vein injection of AAV9-*C1ORF194*, although intravenous administration would be an easier administration route in clinical settings. Nevertheless, this administration route is not without its challenges, including concerns of needle-related complications, potential infections, and the risk of vascular damage. In previous AAV gene therapy studies at CMT, investigators used a variety of virus delivery methods, including intravenous injection [24–26], dorsal root ganglion injection [27, 28], intramuscular injection [29–33], and intrathecal injections [34–39]. Injection of AAV directly into the sciatic nerve has been found to deliver genes directly to Schwann cells and to successfully ameliorate neuropathology in a mouse model of X-linked CMT [27]. However, the utility of translation of this approach to clinical settings is limited by the invasive nature of the technique and the need to inject multiple nerves to achieve a functional therapeutic effect. Injection of viral vectors directly into the dorsal root ganglion increases gene expression in this region; this approach may be effective primarily in disorders dominated by sensory neuropathies [28]. However, because of possible safety hazards, the potential for clinical transformation is limited. Intramuscular injections have been used to indirectly deliver therapeutic and

neuroprotective genes to peripheral nerves. Intramuscular delivery of neurotrophin-3 to the CMT1A model has shown promising efficacy [30, 40].

Although many viral delivery methods are available, intravenous delivery is the most convenient and safe method at the operational level. In the future experiment, we will improve the AAV vector by replacing the current CAG promoter with the myelin-specific myelin protein zero (MPZ) promoter, which is highly selective for Schwann cells [41]. This promoter has been shown to drive transgenic high-level expression of *Cx32* in Schwann cells of *Cx32* knockout mice, thereby completely rescuing the phenotype in this CMT1X model [42]. Furthermore, this promoter has been demonstrated to specifically drive viral vector expression in Schwann cells both in vitro and in vivo. When packaged into lentiviral vectors, durable expression of the transgene in Schwann cells has been achieved after intraneural and intrathecal injection [39, 43]. In our study, the sensory and motor abilities of *C1orf194*$^{-/-}$ mice somewhat improved after intravenous injection of recombinant AAV9-*C1ORF194*. In addition, we aim to identify the mechanism linking *C1orf194* and CMT. In one of our studies, we found that the absence of *C1orf194* as a calcium-regulating factor may lead to abnormalities in multiple systems, including the nervous system, in early embryo development. In future studies, we expect to identify small molecule inhibitors or agonists that target the *C1orf194* pathway, thereby improving CMT specifically caused by the *C1orf194* mutant.

Materials and Methods

Ethics Statement

Animal experiments were approved by the Southern Medical University Laboratory Animal Welfare and Ethics Committee (Guangzhou, China). Specific-pathogen-free mice were reared in a barrier facility under the care of the Laboratory Animal Center (Institute of Comparative Medicine), Southern Medical University, which is accredited by the Association for Assessment and Accreditation of Laboratory Animal Care.

Experimental Plan

All mice were genotyped 15 days after birth (P15). Mice were treated 45 days after birth with a dose of AAV9-*C1ORF194* (5×10 [12] VG, approximately 250μL) via tail vein injection. Our studies involved three groups: WT group, control group (injected with phosphate-buffered saline (PBS)), and experimental group (injected with AAV9-*C1ORF194*), with six mice each. Behavioral characteristics were observed at the ages of 4 and 6 months, and neuro-electrophysiological and histopathological examinations were performed at 6 months of age. In addition, we performed western blotting to detect the expression of C1orf194 in the sciatic nerve in all mice.

Mouse Tissue Harvesting and Processing

Mice were anesthetized and sacrificed by cervical dislocation. The sciatic nerve, gastrocnemius muscle, and spinal cord were dissected and stored at −80 °C for future protein assays. For microscopy, mice anesthetized with 4% PFA ether were perfused with 2.5% glutaraldehyde, and the sciatic nerve was dissected and fixed in glutaraldehyde solution for 4 h and stored in PBS for 12 h. For histologic analysis, the gastrocnemius muscle and spinal cord were dissected from mice after perfusion fixation and postfixed in 4% paraformaldehyde for 6 h.

Western Blotting

The spinal cord, gastrocnemius muscle, and sciatic nerve tissue were homogenized in radioimmunoprecipitation assay buffer (Cell Signaling Technology, Danvers, MA, USA) containing a protease inhibitor cocktail (Sigma-Aldrich, St. Louis, MO, USA). After centrifugation at $14{,}000 \times g$ for 30 min at 4 °C, the supernatant was transferred to a clean microcentrifuge tube. The extracted protein was quantified with a bicinchoninic acid assay (Thermo Fisher Scientific, Waltham, MA, USA) and denatured in protein loading buffer, and then separated by 10% sodium dodecyl sulfate-polyacrylamide gel electrophoresis (Bio-Rad, California, USA) and transferred to a polyvinylidene difluoride membrane (EMD Millipore, Billerica, MA, USA). The membrane was blocked in 5% non-fat milk in PBS-Tween (0.1%) at room temperature for 1 h, and incubated overnight at 4 °C with mouse monoclonal anti-glyceraldehyde 3-phosphate dehydrogenase (Sigma-Aldrich), rabbit polyclonal anti-C1orf194 (Abcam, Cambridge, MA, USA, and Cloud Clone, Wuhan, China), and goat polyclonal anti-700013F07Rik (Santa Cruz Biotechnology, Santa Cruz, CA, USA) antibodies. The membrane was subsequently incubated with horseradish peroxidase-conjugated secondary antibody (Promega) at room temperature for 2 h, and protein bands were visualized with the Enhanced Chemiluminescence ECL Plus kit (Thermo Fisher Scientific) and imaged on an Image-Quant system (GE Healthcare, Wauwatosa, WI, USA).

Behavioral Experiments

To test for amelioration of the CMT phenotype in mice treated with AAV, we performed behavioral tests on the mice. These tests included the hind limb extension test, footprint analysis, rotarod test, grip strength test, and tail flick test. Among them, the tail-flick test indicates sensory ability, whereas the other tests indicate motor ability.

Hind Limb Extension Test

All mice underwent the hind limb extension test at the age of 6 months. Briefly, the mice were suspended by the tail, and hind limb extension was observed for 10 s. A score of 2 corresponded to a normal extension reflex of the hind limbs with splaying of the toes. A score of 1 corresponded to clenching of the hind limbs to the body with partial splaying of the toes. A score of 0 corresponded to clasping the hind limbs with the toes curled. A score of 1.5 or 0.5 corresponded to behaviors between 2 and 1 or 1 and 0, respectively. The test was performed three times at 30-s intervals for each mouse.

Footprint Analysis

The hind paws of the mice were coated with non-toxic black ink, and their footprints were recorded as they walked along a runway (length: 60 cm; width: 5 cm; height: 15 cm) made of clear Perspex. The average stride length (distance of the same foot span in a single step) and stride angle (angle between lines connecting the first toe of footpads from each side of the stride) of at least three consecutive steps were measured, which reflected the walking ability of the mouse [44].

Rotarod Test

Mice were trained for three consecutive days on a rotarod at low speed before the start of the experiment. For the actual experiment, the six stations of the rotarod treadmill were set at a constant speed of 25 rpm, and six mice were tested simultaneously. The time from initial movement on the rotating rod to the time at which the mouse fell off the rod was recorded. Each mouse was tested three times with a 30-min interval between tests. The average time of the three tests was used for statistical analysis. The three groups of mice were tested at 4 and 6 months old.

Grip Strength Test

The mice were placed on a grip-strength apparatus, and their overall limb strength was initially tested. As the mice grasped the apparatus with only their front paws, their tails were gently pulled backward until they released their grip. This procedure was repeated for three consecutive trials. Hindlimb force was calculated by subtraction of the force exerted by the front limbs from the total limb force. Three trials were performed at 20-min intervals for each mouse. The average force of the three tests was used for statistical analysis. The three groups of mice were tested at 4 and 6 months old.

Tail Flick Test

Sensitivity to heat was measured as previously described. Briefly, each mouse was placed in a glass container with its tail exposed to water heated to 52 °C. The temperature was selected on the basis of evidence that it causes slight discomfort, but not pain or injury. The latency before the mouse showed signs of discomfort (flicking, removal of the tail from the water, or jumping) was recorded. Mice that did not show any signs of discomfort after 10 s were removed to prevent injury. The final score was determined by averaging the response times from three trials.

Hematoxylin and Eosin Staining

Six-month-old mice from three groups were perfused with paraformaldehyde solution, and the gastrocnemius muscle was dissected with fine forceps and cut into sections, as previously described. The sections were stained with H&E, and the morphology of the gastrocnemius muscle was examined under a light microscope.

Motor Neuron Counts

The lumbar spinal cord (L1-L5) was removed from 6-month-old mice and embedded in paraffin, and four consecutive sections were cut at a thickness of 5 μm for Nissl staining. Polygonal neurons in the bilateral anterior horns in which the nucleolus was visible were counted at high magnification. Data were obtained from six mice per group as described before [44].

Nissl Staining

Lumbar spinal cord (L1-L5) paraffin samples, with a thickness of 5μm, were subjected to the following steps for staining and observation. First, the samples were placed in a xylene container for several minutes to dissolve the wax. Subsequently, they were treated with varying concentrations of ethanol to eliminate any residual xylene that might potentially interfere with the staining process. Next, the staining solution was added dropwise to the samples, which were then incubated at 37 ℃ for 30 min. After incubation, the samples were thoroughly washed with distilled water. For removal of excess water and ethanol, the samples were sequentially immersed in increasing concentrations of ethanol, and then treated with xylene. Finally, the prepared samples were mounted on slides using neutral resin. The neurons

in the anterior horn of the lumbar spinal cord were observed under a light microscope after Nissl staining.

Electron Microscopy

Distal sciatic nerve segments with lengths of 1–2 mm were collected from three 6-month-old mice per group, fixed in 2.5% glutaraldehyde, and post-fixed in 1% OsO_4. After dehydration in a graded series of acetone, the samples were embedded in epoxy resin and cut into ultra-thin sections (60 nm) that were counterstained with 2% uranyl acetate and lead citrate solution before visualization by transmission electron microscopy. The diameter of the axon and nerve fibers, the thickness of the myelin sheath, and the structures of axons and Schwann cells were evaluated [45, 46].

Electrophysiology

The average CMAP and NCV of the sciatic nerve were recorded in 6-month-old mice as described previously. Briefly, mice were anesthetized by intraperitoneal injection of 10% chloral hydrate according to their body weight. Stimulating and recording electrodes were placed at the sciatic notch and ankle, respectively, and the ground wire was placed at the tail. CMAP and NCV were analyzed with LabChart 7 software (ADInstruments, Bella Vista, Australia).

Statistical Analysis

Statistical analyses were performed with GraphPad8 software. Statistical differences among the three groups were determined with one-way ANOVA analysis of variance followed by Bernoulli correction. Statistical differences between two groups were determined with independent samples *t*-test. Data are presented as the mean and standard error of the mean. For all analyses, statistical significance is denoted as $*P<0.05$, $**P<0.01$, or $***P<0.001$.

Acknowledgements The authors thank the patients for supporting previous research that facilitated the generation of this manuscript. We thank International Science Editing (http://www.internationalscienceediting.com) for editing this manuscript.

Funding This work was supported by the National Natural Science Foundation of China (32170617 and 31970558), National Key S&T Special Projects (2021YFC100530 and 2022YFC2703303), and Natural Science Foundation of Guangdong Province of China (2022A1515012621).

Declarations

Conflict of Interest All authors report no conflicts of interest. The study sponsors had no role in any stage of this work.

References

1. Hattori N, Yamamoto M, Yoshihara T, Koike H, Nakagawa M, Yoshikawa H, et al. Demyelinating and axonal features of Charcot–Marie–Tooth disease with mutations of myelin-related proteins (PMP22, MPZ and Cx32): a clinicopathological study of 205 Japanese patients. Brain. 2003;126:134–51.
2. Berciano J, García A, Gallardo E, Peeters K, Pelayo-Negro AL, Álvarez-Paradelo S, et al. Intermediate Charcot–Marie–Tooth disease: an electrophysiological reappraisal and systematic review. J Neurol. 2017;264:1655–77.
3. Sun S-C, Ma D, Li M-Y, Zhang R-X, Huang C, Huang H-J, et al. Mutations in C1orf194, encoding a calcium regulator, cause dominant Charcot-Marie-Tooth disease. Brain. 2019;142:2215–29.
4. Huang C, Shen ZR, Huang J, Sun SC, Ma D, Li MY, et al. C1orf194 deficiency leads to incomplete early embryonic lethality and dominant intermediate Charcot–Marie–Tooth disease in a knockout mouse model. Hum Mol Genet. 2020;29:2471–80.
5. Berciano J, García A, Combarros O. Initial semeiology in children with Charcot-Marie-Tooth disease 1A duplication: CMT-1A Initial Semeiology. Muscle Nerve. 2003;27:34–9.
6. Krajewski K, Lewis R, Fuerst D, Turansky C, Hinderer S, Garbern J, et al. Neurological dysfunction and axonal degeneration in Charcot-Marie-Tooth disease type 1A. J Peripher Nerv Syst. 2001;6:61–61.
7. Bird TD. Charcot-Marie-Tooth hereditary neuropathy overview. University of Washington, Seattle, 2022. https://www.ncbi.nlm.nih.gov/books/NBK1358/. (Accessed 13 Jan 2023).
8. Morena J, Gupta A, Hoyle JC. Charcot-Marie-Tooth: from molecules to therapy. Int J Mol Sci. 2019;20:3419.
9. Padua L, Aprile I, Cavallaro T, Commodari I, La Torre G, Pareyson D, et al. Handgrip impairment in Charcot-Marie-Tooth disease. Eura Medicophys. 2006;27:417–23.
10. Sman AD, Hackett D, Fiatarone Singh M, Fornusek C, Menezes MP, Burns J. Systematic review of exercise for Charcot-Marie-Tooth disease. J Peripher Nerv Syst. 2015;20:347–62.
11. Guyton GP. Orthopaedic aspects of Charcot-Marie-Tooth disease. Foot Ankle Int. 2006;27:1003–10.
12. Chan G, Bowen JR, Kumar SJ. Evaluation and treatment of hip dysplasia in Charcot-Marie-Tooth disease. Orthop Clin North Am. 2006;37:203–9.
13. Corrado B, Ciardi G, Bargigli C. Rehabilitation management of the Charcot–Marie–Tooth syndrome. Medicine (Baltimore). 2016;95: e3278.
14. Kenis-Coskun O, Matthews DJ. Rehabilitation issues in Charcot-Marie-Tooth disease. J Pediatr Rehabil Med. 2016;9:31–4.
15. Mendell JR, Al-Zaidy S, Shell R, Arnold WD, Rodino-Klapac LR, Prior TW, et al. Single-dose gene-replacement therapy for spinal muscular atrophy. N Engl J Med. 2017;377:1713–22.
16. White KA, Nelvagal HR, Poole TA, Lu B, Johnson TB, Davis S, et al. Intracranial delivery of AAV9 gene therapy partially prevents retinal degeneration and visual deficits in CLN6-Batten disease mice. Mol Ther - Methods Clin Dev. 2021;20:497–507.
17. Mendell JR, Al-Zaidy SA, Lehman KJ, McColly M, Lowes LP, Alfano LN, et al. Five-year extension results of the phase 1 START trial of onasemnogene abeparvovec in spinal muscular atrophy. JAMA Neurol. 2021;78:1–8.
18. Mendell JR, Sahenk Z, Lehman K, Nease C, Lowes LP, Miller NF, et al. Assessment of systemic delivery of rAAVrh74. MHCK7.micro-dystrophin in children with Duchenne muscular dystrophy. JAMA Neurol. 2020;77:1–10.
19. Wang D, Zhong L, Nahid MA, Gao G. The potential of adeno-associated viral vectors for gene delivery to muscle tissue. Expert Opin Drug Deliv. 2014;11:345–64.

20. Bish LT, Morine K, Sleeper MM, Sanmiguel J, Wu D, Gao G, et al. Adeno-associated virus (AAV) serotype 9 provides global cardiac gene transfer superior to AAV1, AAV6, AAV7, and AAV8 in the mouse and rat. Hum Gene Ther. 2008;19:1359–68.
21. Su H, Yeghiazarians Y, Lee A, Huang Y, Arakawa-Hoyt J, Ye J, et al. AAV serotype 1 mediates more efficient gene transfer to pig myocardium than AAV serotype 2 and plasmid. J Gene Med. 2008;10:33–41.
22. Stavrou M, Kagiava A, Sargiannidou I, Georgiou E, Kleopa KA. Charcot–Marie–Tooth neuropathies: current gene therapy advances and the route toward translation. J Peripher Nerv Syst. 2023;28:150–68.
23. Al-Zaidy SA, Kolb SJ, Lowes L, Alfano LN, Shell R, Church KR, et al. AVXS-101 (onasemnogene abeparvovec) for SMA1: comparative study with a prospective natural history cohort. J Neuromuscul Dis. 2019;6:307–17.
24. Gautier B, Hajjar H, Soares S, Berthelot J, Deck M, Abbou S, et al. AAV2/9-mediated silencing of PMP22 prevents the development of pathological features in a rat model of Charcot-Marie-Tooth disease 1 A. Nat Commun. 2021;12:2356.
25. Lee J-S, Lee JY, Song DW, Bae HS, Doo HM, Yu HS, et al. Targeted PMP22 TATA-box editing by CRISPR/Cas9 reduces demyelinating neuropathy of Charcot-Marie-Tooth disease type 1A in mice. Nucleic Acids Res. 2020;48:130–40.
26. Boutary S, Caillaud M, El Madani M, Vallat J-M, Loisel-Duwattez J, Rouyer A, et al. Squalenoyl siRNA PMP22 nanoparticles are effective in treating mouse models of Charcot-Marie-Tooth disease type 1 A. Commun Biol. 2021;4:1–14.
27. Sargiannidou I, Kagiava A, Bashiardes S, Richter J, Christodoulou C, Scherer SS, et al. Intraneural GJB1 gene delivery improves nerve pathology in a model of X-linked Charcot–Marie–Tooth disease. Ann Neurol. 2015;78:303–16.
28. Pleticha J, Maus TP, Christner JA, Marsh MP, Lee KH, Hooten WM, et al. Minimally invasive convection-enhanced delivery of biologics into dorsal root ganglia: validation in the pig model and prospective modeling in humans: Technical note. J Neurosurg. 2014;121:851–8.
29. Ozes B, Moss K, Myers M, Ridgley A, Chen L, Murrey D, et al. AAV1.NT-3 gene therapy in a CMT2D model: phenotypic improvements in GarsP278KY/+ mice. Brain Commun. 2021;3:fcab252.
30. Sahenk Z, Galloway G, Clark KR, Malik V, Rodino-Klapac LR, Kaspar BK, et al. AAV1.NT-3 gene therapy for Charcot–Marie–Tooth neuropathy. Mol Ther. 2014;22:511–521.
31. Burst mitofusin activation reverses neuromuscular dysfunction in murine CMT2A - PMC. https://www.ncbi.nlm.nih.gov/pmc/articles/PMC7655101/. (Accessed 22 Jul 2023).
32. Rocha AG, Franco A, Krezel AM, Rumsey JM, Alberti JM, Knight WC, et al. Mfn2 agonists reverse mitochondrial defects in preclinical models of Charcot Marie Tooth disease type 2A. Science. 2018;360:336–41.
33. Thomas FP, Brannagan TH, Butterfield RJ, Desai U, Habib AA, Herrmann DN, et al. Randomized phase 2 study of ACE-083 in patients with Charcot-Marie-Tooth disease. Neurology. 2022;98:e2356–67.
34. A translatable RNAi-driven gene therapy silences PMP22/Pmp22 genes and improves neuropathy in CMT1A mice - PMC. https://www.ncbi.nlm.nih.gov/pmc/articles/PMC9246392/. (Accessed 22 Jul 2023).
35. Kagiava A, Karaiskos C, Richter J, Tryfonos C, Jennings MJ, Heslegrave AJ, et al. AAV9-mediated Schwann cell-targeted gene therapy rescues a model of demyelinating neuropathy. Gene Ther. 2021;28:659–75.
36. Allele-specific RNA interference prevents neuropathy in Charcot-Marie-Tooth disease type 2D mouse models - PMC. https://www.ncbi.nlm.nih.gov/pmc/articles/PMC6877339/. (Accessed 22 Jul 2023).
37. Development of Intrathecal AAV9 Gene Therapy for Giant Axonal Neuropathy - PMC. https://www.ncbi.nlm.nih.gov/pmc/articles/PMC5948230/. (Accessed 22 Jul 2023).
38. Kagiava A, Richter J, Tryfonos C, Karaiskos C, Heslegrave AJ, Sargiannidou I, et al. Gene replacement therapy after neuropathy onset provides therapeutic benefit in a model of CMT1X. Hum Mol Genet. 2019;28:3528–42.
39. Schiza N, Georgiou E, Kagiava A, Médard J-J, Richter J, Tryfonos C, et al. Gene replacement therapy in a model of Charcot-Marie-Tooth 4C neuropathy. Brain. 2019;142:1227–41.
40. Yalvac ME, Amornvit J, Chen L, Shontz KM, Lewis S, Sahenk Z. AAV1.NT-3 gene therapy increases muscle fiber diameter through activation of mTOR pathway and metabolic remodeling in a CMT mouse model. Gene Ther. 2018;25:129–138.
41. Messing A, Behringer R, Hammang JP, Palmiter RD, Brinster RL, Lemke G. P0 promoter directs expression of reporter and toxin genes to Schwann cells of transgenic mice. Neuron. 1992;8:507–20.
42. Scherer SS, Xu Y-T, Messing A, Willecke K, Fischbeck KH, Jeng LJB. Transgenic expression of human connexin32 in myelinating Schwann cells prevents demyelination in connexin32-null mice. J Neurosci. 2005;25:1550–9.
43. Kagiava A, Sargiannidou I, Theophilidis G, Karaiskos C, Richter J, Bashiardes S, et al. Intrathecal gene therapy rescues a model of demyelinating peripheral neuropathy. Proc Natl Acad Sci. 2016;113:E2421–9.
44. Barneo-Muñoz M, Juárez P, Civera-Tregón A, Yndriago L, Pla-Martin D, Zenker J, et al. Lack of GDAP1 induces neuronal calcium and mitochondrial defects in a knockout mouse model of Charcot-Marie-Tooth neuropathy. PLOS Genet. 2015;11:e1005115.
45. Arnold WD, Sheth KA, Wier CG, Kissel JT, Burghes AH, Kolb SJ. Electrophysiological motor unit number estimation (MUNE) measuring compound muscle action potential (CMAP) in mouse hindlimb muscles. J Vis Exp. 2015;52899.
46. Schulz A, Walther C, Morrison H, Bauer R. In vivo electrophysiological measurements on mouse sciatic nerves. J Vis Exp. 2014;51181.